Formation Flying Interferometry

Oliver Lay & Gary Blackwood
Jet Propulsion Laboratory, 4800 Oak Grove Drive, Pasadena CA 91109

ABSTRACT

There are many advantages to space-based interferometry, but monolithic, single-spacecraft platforms set limits on the collecting area and baseline length. These constraints can be overcome by distributing the optical elements of the interferometer over a system of multiple spacecraft flying in precise formation, opening up new realms of angular resolution and sensitivity.

While the principles of interferometry are the same as for structurally connected systems, formation flying interferometers must integrate a wide range of technologies to provide an optically stable platform capable of finding, tracking and measuring fringes. This paper discusses some of the key differences between formation flying and structurally connected interferometers, including formation configurations, controlling beam shear, station-keeping, and the importance of delay and delay rate estimation in determining the instrument sensitivity.

Proposed future formation flying interferometer missions include the Terrestrial Planet Finder (TPF), Darwin, the Submillimeter Probe of the Evolution of Cosmic Structure (SPECS), the Stellar Imager, the Micro-Arcsecond Xray Imaging Mission (MAXIM), and its precursor, MAXIM Pathfinder. In addition, Life Finder and Planet Imager have been identified as two formation flying missions capable of detailed characterization of habitable exo-planets. The parameters for these missions are compared and described briefly.

Keywords:

1. INTRODUCTION

Many of the long-term objectives for observational astronomy demand unprecedented angular resolution at sensitivity, from radio to X-Ray wavelengths, and beyond the electromagnetic spectrum to gravity waves. The scope of this paper is restricted to interferometers based on direct (homodyne) detection of light, and therefore does not discuss gravitational wave missions such as LISA (Laser Interferometer Space Antenna), or space-based radio telescope arrays such as ARISE (Advanced Radio Interferometry between Space and Earth).

Interferometers coherently combine the light from two or more collecting apertures to achieve an angular resolution approximately equivalent to a single aperture with diameter equal to the baseline between the collectors. High angular resolution requires long baselines, and high sensitivity requires a large collecting area; both are limited by the mass and size constraints of a single spacecraft platform. The Next Generation Space Telescope is planned to have an aperture diameter of 6 m, and the Space Interferometry Mission will have a baseline of 10 m. Deployable booms of 50 – 100 m in length are being considered, but meeting long-term objectives such as detailed imaging of nearby stellar surfaces, black hole event horizons, and terrestrial planets requires baselines that can only be achieved using separated spacecraft.

In a Formation Flying Interferometer (FFI) the collecting apertures and beam combination optics are distributed across two or more spacecraft. The primary advantages to this approach are threefold: (1) much longer baselines are possible than for single spacecraft, (2) the baseline length is continuously adjustable (good for imaging) and can be tuned to an optimal length (good for planet-finding), (3) the total collecting area can be much larger than for a single spacecraft. Secondary: long focal length (X-Ray). There are many challenges to be overcome, however. New technologies for precision formation flying are needed, including sensors, precision thrusters and robust control algorithms. Laser metrology systems must operate over long ranges with great precision. Fundamentally new approaches are needed for mission operations and fault protection. Rather than focus on these issues, most of which have been discussed elsewhere, this paper will focus on some of the key differences between formation flying interferometers and those that are attached to fixed structures (the Earth or single spacecraft): the choice of configuration (i.e. distribution of collecting apertures), the control of beam shear, station-keeping requirements and the key role of estimating delay and delay rate in determining the sensitivity. The final section contains a summary of formation flying interferometers planned for the future. First, it is useful to classify the different interferometer observing modes.

2. INTERFEROMETRY & PHASE REFERENCING

Astronomical interferometers have been operated in four basic modes of observation: imaging, nulling, astrometry and visibility amplitude. The description given in this section applies to all interferometers.

Imaging mode is used to synthesize the target brightness distribution by measuring many spatial Fourier components. Observations of the fringe visibility amplitude and phase are made at each of a large number of baselines. The number of baselines needed depends on the complexity and extent of the target.

Nulling mode is analogous to coronography for single aperture telescopes; the goal is to image the area immediately surrounding a bright target, but to suppress the light from central target itself. It is a special case of imaging. The prime example is the search for planets around nearby stars. The dynamic range in brightness may be 10^6 or more for an Earth-like planet, and nulling of the central star is essential to reduce the level of noise. The technique of nulling is described elsewhere in this is conference (references).

Astrometry mode measures the angular offsets between target objects on the sky. This technique is described elsewhere in this conference (references).

Visibility amplitude mode is the equivalent of imaging without the visibility phase information, and can be used when the target is relatively bright and has a simple structure. Examples include the measurement of stellar diameters and close binary separations.

If the geometry of an interferometer (baseline vector and internal path lengths) is fixed with respect to inertial space, then the optical path difference for the beams propagating from the target through the instrument to the combiner is stable (assuming there is no atmosphere), and it is possible to integrate indefinitely to observe arbitrarily faint targets. Static geometry is not a necessary condition, since an adjustable delay line can compensate for known motions. Large uncertainty in the motion gives a low coherence time for the interferometer and low sensitivity. Changes in the baseline length and internal path lengths can be measured with laser metrology; it is the orientation of the baseline vector with respect to inertial space that poses the challenge. Two techniques have been proposed: phase referencing to guide stars and the use of gyroscopes. The latter have been used extensively on single spacecraft platforms to measure the rate of change of inertial attitude. Although the performance of these self-contained units is not sufficient for most interferometry needs, the concept has been extended recently to the optical ring gyro, where counter-propagating laser beams circulate around the formation, and the phase of the interfered beams is very sensitive to the orientation of the formation (reference Roger memo and paper at conference, 1998 SPIE paper?).

Phase referencing to bright, compact guide stars can be used to obtain the rotation rate of the baseline vector. Fringes are tracked simultaneously on one or two guide stars, using the same baseline vector as that for the science target. Rotation of the baseline vector results in motion of the guide star fringes, which are tracked and fed forward to the science delay line, thereby stabilizing the fringes on the science target. There are 3 regimes of phase referencing, defined by the offset of the guide star relative to the science target:
(1) *Self-calibration*: the target object itself is bright and compact enough to find and track fringes on.
(2) *Narrow-angle phase referencing*: fringes are tracked on a bright, compact object that lies within the field of view of the collector telescopes. For interferometers using pupil plane combination (aka Michelson interferometers) the target and guide light is separated the collector telescopes and transported as 2 separate beams for combination. The guide star beam will require a modest delay correction relative to the science beam (reference). Interferometers using image plane combination (aka Fizeau interferometers) can form fringes in the focal plane on both science and guide star, provided the pupil geometry is preserved (reference). In either case, the science target must be close on the sky to a guide star of sufficient brightness to find and track fringes.
(3) *Wide-angle phase referencing*: separate collector telescopes, paired up structurally with the science telescopes, are used to observe a pair of guide stars that may be separated by many degrees from the science target. Three beam trains

are now needed (one science, two guide) with substantial delay compensation before beam combination. This extra complexity enables the observation of faint science targets anywhere on the sky.

Table 1 shows the combinations of interferometer observing modes and phase referencing scheme. In the case of nulling, the bright, compact star to be nulled can be used for fringe tracking

	Interferometry Observing Mode			
Phase referencing scheme	Imaging	Nulling	Astrometry	Visibility amplitude
1. Self-referencing	Bright targets only	Bright targets		Bright targets only
2. Narrow-angle referencing	Limited number of faint targets		Narrow-angle astrometry	
3. Wide-angle referencing	Any target		Wide-angle astrometry	

Table 1: Interferometry Observing Modes

The number of targets accessible to self- and narrow-angle referencing depends on the faintest target for which fringes can be found and tracked. As described quantitatively in Section 6, this limiting magnitude depends on the uncertainty in the baseline rotation rate, the size and quality of the optics and the spectral resolution of the instrument. The probability of finding a sufficiently bright guide star within a small radius of the science target increases rapidly with the limiting magnitude. The future missions described in Section 7 are almost all focused on observing relatively bright targets, using self- or narrow-angle referencing. One reason for this is the constraints on configuration inherent to formation flying interferometers.

3. CONFIGURATIONS AND PATH EQUALIZATION

Forming interference fringes requires equalization of the path lengths from the target to the beam combiner. A fundamental difference between formation flying and structurally connected interferometers is the capacity to carry long delay lines for path compensation. An interferometer with a baseline of 10 m attached to a boom can have external delays varying between ±10 m, depending on the location of the target with respect to the baseline vector. The internal delay required for compensation can be accommodated within the 10 m long structure. It is much more challenging to accommodate long, adjustable delay lines within a formation flying system, where the baseline lengths may be hundreds of meters and the individual spacecraft are only a few meters across. Formation flying configurations must therefore be chosen such that the path lengths are intrinsically balanced. Figure 1 illustrates some examples.

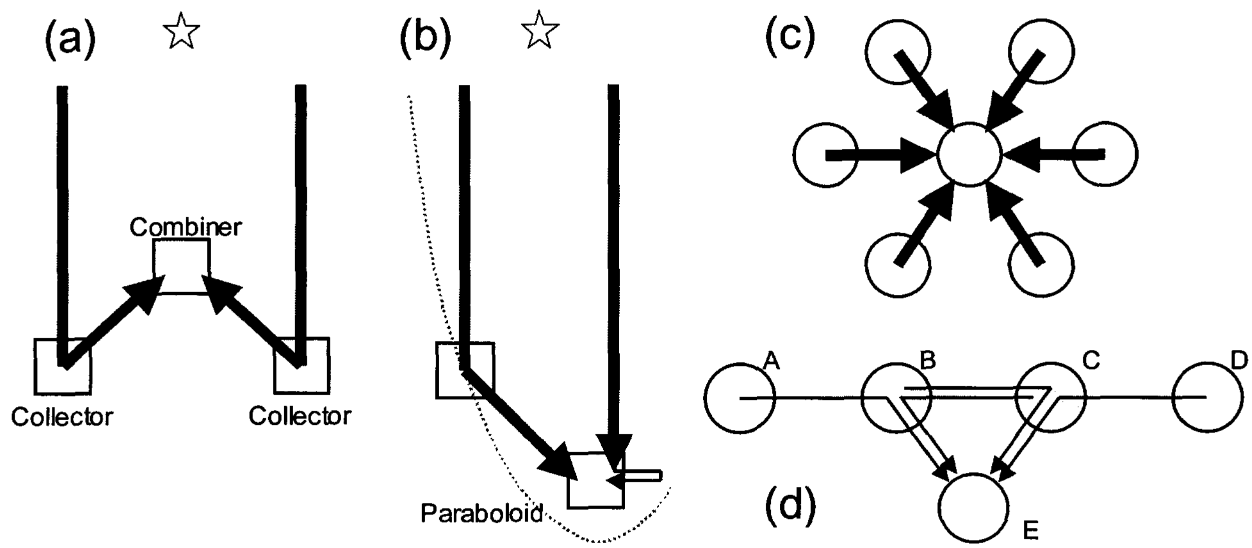

Figure 1: Some formation flying interferometer configurations. (a) Original symmetric 3-spacecraft design for the StarLight mission. (b) Asymmetric 2-spacecraft design for StarLight. The external path imbalance is compensated by a fixed 14 m delay line in the combiner spacecraft. The path lengths remain balanced as long as the collector is on the paraboloidal surface with the combiner at the focus (further references). (c) A proposed configuration for the DARWIN interferometer, with 6 collectors and a central beam combiner. The target star is normal to the plane of the page. (d) Proposed configuration for Terrestrial Planet Finder mission. The path lengths from the collectors (A, B, C, D) to the combiner E are balanced if the collectors are equally spaced along a line and BE = CE.

Balancing path lengths in a design where there is direct propagation from each collector to the combiner requires that the collectors lie on a paraboloidal surface whose axis is in the direction of the star and with the combiner at the focus. In general, the focal length of this paraboloid is not constrained (e.g. the combiner can be moved toward or away from the star in Fig. 1(a) and (c)). An exception is the 2-spacecraft StarLight design, where the focal length of the paraboloid (vertex to focus) is half the length of the compensating fixed delay.

With 2 collectors, the path lengths are balanced for any target with direction perpendicular to the baseline – a great circle on the sky. Switching between two targets on this circle requires only a change in orientation of the individual spacecraft. A target and guide star on the great circle could be observed simultaneously (either narrow- or wide-angle) without additional delay compensation. For the wide-angle case, two guide stars are needed on or close to the great circle. With 3 or more collectors the path lengths can only be balanced geometrically for one target at a time. The long delay lines needed for wide-angle phase referencing would require either a highly folded bulk optics delay, a fiber delay line, separate combiner spacecraft for the target and each guide star, or additional spacecraft to house the far end of adjustable reflective delay lines.

An alternative approach is shown in Fig. 1(d), where the paths are balanced using a "2-hop" propagation from each collector to the combiner. The collectors must be equally spaced, leading to some redundancy. The baselines can be expanded while preserving the angles.

There are other considerations in choosing configurations. At mid- and far-infrared wavelengths it is important to cool the collector optics. Planar configurations are preferred, since it avoids the illumination of cold optics by the warm, solar-illuminated underside of one of the other spacecraft. This becomes less of an issue as the separations are increased. At X-Ray wavelengths, all reflections must be made close to grazing incidence, where the roughness of the optical surfaces has minimal impact on the wavefront. As a result, the combiner spacecraft must located at a very long distance from the collectors. A configuration for the MAXIM mission deploys the collectors in a ring of diameter 100 m, with the combiner spacecraft located on the axis a further 500 km along the direction from the target. However, a large formation like this will require substantially more energy for retargeting, compared to the equivalent planar configuration with diameter 100 m.

4. CONTROLLING BEAM SHEAR

An important difference between Structurally Connected and Formation Flying interferometers is the need to control beam shear. The situation is illustrated in Fig. 2. Once the Structurally Connected case (Fig. 2a) is correctly aligned, the beam shear at the input to the combiner is zero as long as the angle-tracking control loop is correctly tracking the target by adjusting the tip/tilt at the collector. When the structural connections are removed (Fig. 2b), the combiner and collectors can be translated relative to one another along the direction to the target, whilst preserving the directions of the beams. The angle-tracking control loops do not sense this translation, but large beam shears are introduced at the combiner inputs.

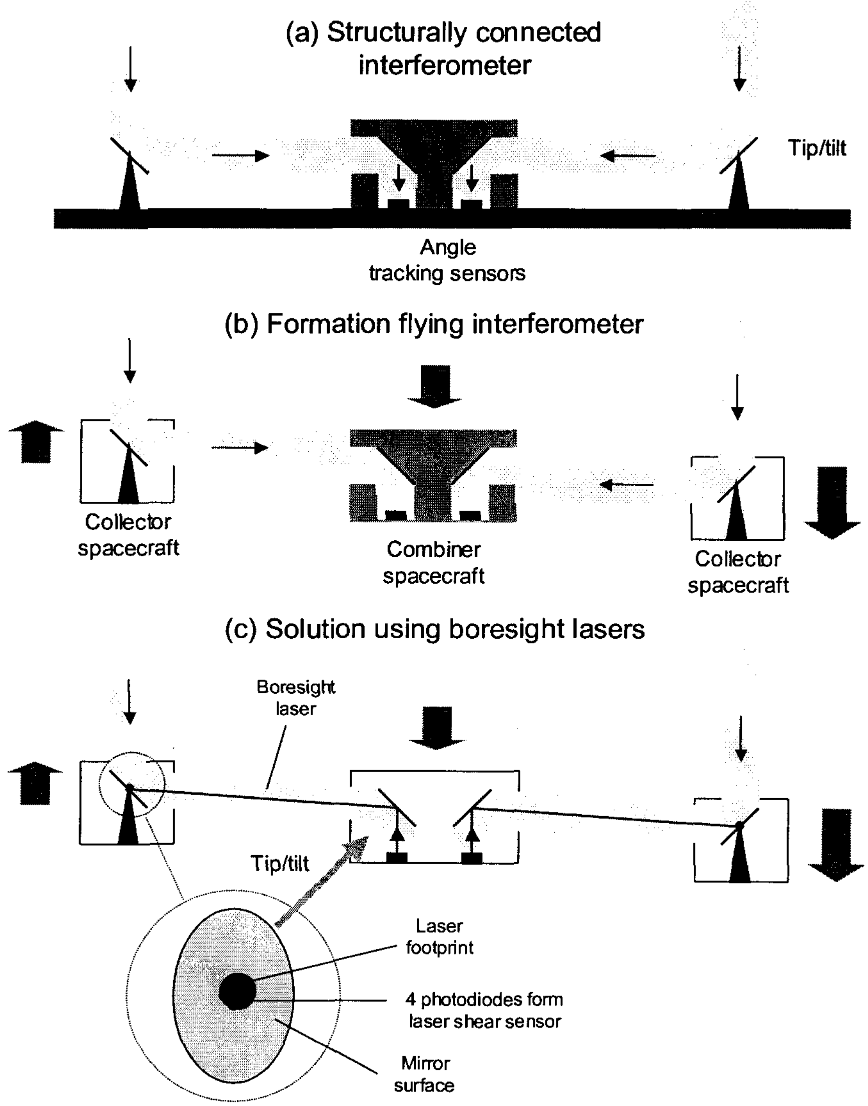

Figure 2: Schematic illustration of the beam shear problem for formation flying interferometers. (a) Simple Structurally Connected Interferometer with two collectors and a combiner. The beam combination optics are omitted for clarity. (b) Formation Flying version showing how translations of the combiner and collectors along the target direction introduce beam shear at the combiner. (c) Beam shear control using boresight lasers and laser shear sensors at the collectors.

One simple solution to this problem is illustrated in Fig. 2c. Boresight lasers, injected outwards at the beam combiner optics are kept pointed at the centers of the collector optics. Offsets in the laser footprints are sensed using a set of 4 photodiodes, configured as a quadrant detector, and corrected using tip/tilt mirrors on the combiner. Further details on how this system was implemented on the StarLight mission can be found in (Riley paper). A different approach is to "rigidize" the formation by forming an optical truss of laser metrology beams between the spacecraft and tightly control the relative positions and orientations to maintain a fixed geometry.

In either case, it is necessary to close control loops that are distributed across different spacecraft. Each angle tracking loop has a sensor on the combiner and an actuator on the collector. Each shear control loop has a sensor on the collector and an actuator on the combiner. The inter-spacecraft communication links must provide low latency, and data rates sufficient to support these loops.

5. STATION-KEEPING

The relative positions and attitudes of the spacecraft within a formation are constantly perturbed by gravitational gradients, solar radiation pressure, and the finite control authority of the formation flying system (imperfect sensors, minimum impulse from actuators). Angle-tracking and beam shear control in a dynamic formation were described above; in addition the path lengths from the target to the beam combiner must be kept equal. Station-keeping applies to the inertial attitudes of each spacecraft, as well as their relative positions. The tolerances required depend on the ranges of the actuators available for compensation. In Fig. 2c the articulation ranges of the tip/tilt mirrors, both at the collectors and the combiner, constrain the angular deformations of the formation and the allowed rotations of the individual spacecraft. The length of the delay line (not shown) constrains the relative separations of the spacecraft and translations along the target direction. There may also be other constraints specific to the mode of observation; in the case of nulling, fro example, tight symmetry in the propagation paths is desirable. The important point is that a formation flying interferometer does not have to be a totally "rigid" entity; flexibility in the motion can be compensated internally, provided there is sufficient knowledge of the distortions, and formation control can be traded against the range of the compensating actuators.

Actuator	Description	Pros	Cons
Thrusters	Many types available. e.g. chemical, cold gas, Pulsed Plasma Thrusters (PPT), Field Emission Effect Propulsion System (FEEPS)	- Can provide attitude and translation control	- Micro-Newton thrusts possible - Consumable propellant - Contamination of optical surfaces - Plumes
Reaction wheels	Electrically driven wheels. Wheel spun up one way, spacecraft turns the other way.	- Established technology	- No translation control - Source of vibration
Tethers	Cables connecting spacecraft which can be paid out or pulled in to control separation	- Saves fuel	- Prevents "evaporation" - Still need thrusters for control - Tether management issues - Source of stray light
Electro-magnets	Powerful electromagnets on each spacecraft provide mutual attraction/repulsion	- Saves fuel - No contamination	- Currently just a concept - Less effective at large separations
Solar sails	Forces generated by momentum of solar photons impinging on large reflective sails	- Saves fuel - No contamination	- Very immature - Low thrust

Table 2: Summary of different approaches to station-keeping

Figure 3: compare control and knowledge requirements to other missions

6. DELAY AND DELAY RATE ESTIMATION AND SENSITIVITY

Section 1 alluded to the importance of baseline rotation knowledge in determining the sensitivity of an interferometer, a concept that is developed more quantitatively in this section, to obtain an approximate expression for the faintest target for which fringes can be using a formation flying interferometer. Figure 4 shows the geometry for a simple formation flying system, with two collectors and a combiner.

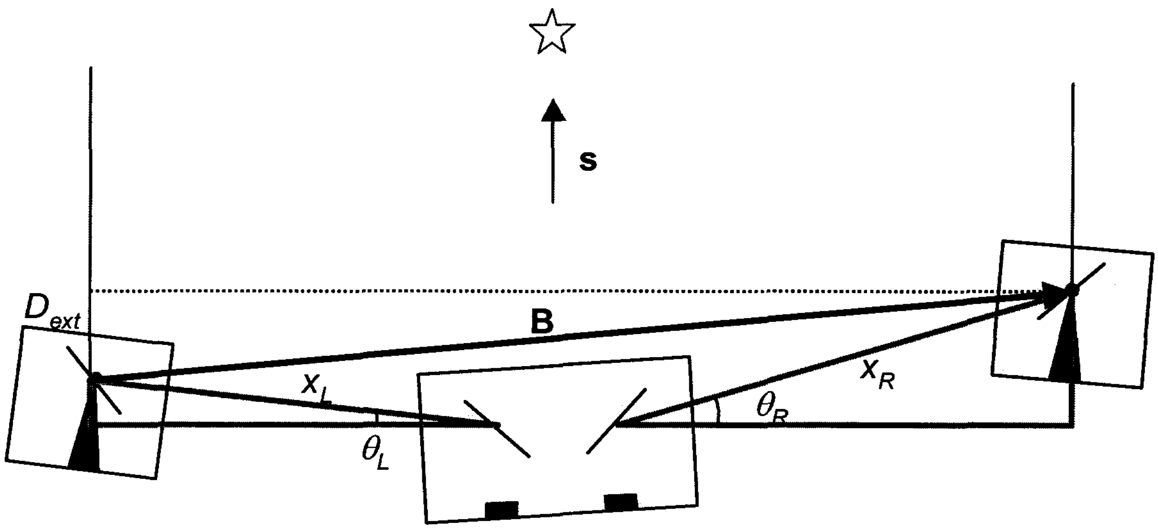

Figure 4: Geometry for simple formation flying system with 2 collectors and a combiner in a linear configuration.

The optical path difference between the left and right paths – the delay – is given by

$$\begin{aligned} D &= D_{\text{ext}} - D_{\text{int}} \\ &= (\mathbf{B}\cdot\mathbf{S}) - (x_L - x_R - D_{\text{off}}) \end{aligned} \tag{1.1}$$

Where D_{ext} and D_{int} are the external and internal delay, respectively, and D_{off} is the delay offset within the combiner spacecaft. For a ground-based interferometer, x_L, x_R and the length of **B** are all fixed, and the inertial orientation of B is a well known function of time. The delay error for a formation flying system can be written as

$$\begin{aligned} \Delta D &= \Delta D_{ext} - \Delta D_{int} \\ &\approx (x_L \Delta\theta_L - x_R \Delta\theta_R) - (\Delta x_L - \Delta x_R - \Delta D_{\text{off}}) \end{aligned} \tag{1.2}$$

Knowledge of the external delay is dominated by uncertainty in the angles θ_L and θ_R. The internal delay requires the measurement of lengths only, which can be accomplished by ranging sensors.

Example calculation for size of the delay error

Differentiating this expression gives the error in the delay rate:

$$\Delta\dot{D} \approx (x_L \Delta\dot{\theta}_L - x_R \Delta\dot{\theta}_R) - (\Delta\dot{x}_L - \Delta\dot{x}_R - \Delta\dot{D}_{\text{off}}) \approx x_L \Delta\dot{\theta}_L - x_R \Delta\dot{\theta}_R \tag{1.3}$$

Measurements of the rate of change of x_L, x_R and D_{off} are readily made at the sub-micron-per-second level with a laser metrology system, so the delay rate error will typically be dominated by estimation of the external delay rate, effectively the rate at which the baseline vector is rotating relative to the target direction. If $x_L \sim x_R \sim x$, then the uncertainty in the delay rate is given by

$$\sigma_{\dot{D}} \approx \sqrt{2} x \sigma_{\dot{\theta}} . \tag{1.4}$$

Now consider the fringe search process. Assume that the total optical bandwidth available for fringe detection, $\Delta\nu$, is divided into n spectral channels of width $\delta\nu$, with photon rates of R_n and R_l, respectively. The fringe envelope for a given channel has a width in delay space of approximately $c/\delta\nu$. The average dwell time on the fringe, T, given the delay rate uncertainty can be no more than

$$T \square \frac{\text{fringe envelope width}}{\text{delay rate uncertainty}} \square \frac{c/\delta\nu}{\sqrt{2}x\sigma_{\dot{\theta}}}. \tag{1.5}$$

In practice, this expression for dwell time is generous, since an effective fringe search requires a search speed a few times higher than the delay rate uncertainty to ensure that the fringe cannot "outrun" the search. The Signal-to-Noise Ratio for fringe detection in a single spectral channel is given by

$$SNR_1 \square \frac{R_1 T V}{\sqrt{R_1 T + 4\frac{\nu}{\delta\nu} r^2}}, \tag{1.6}$$

where V is the fringe visibility amplitude. The first term in the denominator corresponds to shot noise; the second is the read noise for a CCD-like detector with read noise r. The number of fringes within the fringe envelope is approximately $\nu/\delta\nu$, and each fringe needs to be sampled about 4 times by the detector, giving a total of $4\nu/\delta\nu$ reads of the fringe. Assuming the measurements of the n spectral channels are combined coherently, the overall signal to noise ratio is

$$SNR_n \square \sqrt{n} \cdot SNR_1. \tag{1.7}$$

There are two regimes of interest, depending on which noise term is dominant:

$$SNR_n \square \left(\frac{nR_n c}{\sqrt{2}x\sigma_{\dot{\theta}}} \right)^{1/2} V \qquad R_1 T \square\ 4\frac{\delta\nu}{\nu} r^2 \tag{1.8}$$

$$SNR_n \square \frac{R_n c}{2x\sigma_{\dot{\theta}} r\sqrt{2\nu\Delta\nu}} V \qquad R_1 T \square\ 4\frac{\delta\nu}{\nu} r^2 \tag{1.9}$$

The first case is where the photon noise dominates the read noise. The SNR increases with the square root of the number of spectral channels. It continues to do so until the read noise becomes dominant, as shown in the second case. This is now independent of the number of spectral channels. For sensitive fringe detection it is important to have a sufficient number of spectral channels to be in the read-noise dominated regime.

A signal-to-noise ratio of approximately 5 is needed for initial fringe detection, to minimize false positives. Equation 9 can then be rearranged to give

$$R_n \square \frac{10x\sigma_{\dot{\theta}} r\sqrt{2\nu\Delta\nu}}{cV}. \tag{1.10}$$

The photon rate required for detection increases in proportion to the length of the baseline, the uncertainty in the rate of change of the baseline orientation and the detector read noise.

For example, consider an optical interferometer with 200 m baseline (x = 100 m), a passband of 0.5 – 1.0 μm ($\Delta\nu = 3 \times 10^{14}$ Hz; $\nu \sim 4 \times 10^{14}$ Hz), and a detector read noise of 3 electrons. If the angular rates are measured with an uncertainty of 10 milliarcsec/s (= 50 nrad/s), and the fringe visibility V =0.5, then the total photon rate required at the detector is $R_n \sim$ 500 / s. In addition, if the interferometer has two collecting apertures with diameter 1 m, and 10% of the incident photons reach the detector, then it can be shown that the target must have a relative magnitude of 17 or less to find fringes. This would set a limit on the dimmest target accessible to self-calibration, or the dimmest guide stars that could be used for narrow- or wide-angle referencing (Table 1).

For a given uncertainty in the angle rate, the limiting magnitude decreases (i.e. gets brighter) with the baseline length. In a configuration with many collectors, it would be easiest to acquire fringes on the short baselines first (in addition to the delay rate estimation, the target may also have a higher visibility). For example, if fringes are being tracked on short baselines between collectors 1 and 2 and between collectors 2 and 3, then the longer baseline between 1 and 3 is automatically co-phased. Alternatively, for a formation flying interferometer with two collectors, fringes could be found on a short baseline, and then tracked as the baseline length is gradually increased.

The angles θ_L and θ_R can be determined from the deviation angle of the incoming starlight beams at each collector. This in turn is determined by the orientation of the collector optics, relative to the target direction. Figure 4 is a particularly simple example with a single plane mirror at each collector; if the orientations of the collector spacecraft are known relative to the target direction (using an acquisition camera at each collector, for example) then the encoder reading for the in-plane tilt of the mirror gives the deviation angle.

Optical gyroscopes have been proposed as a means to measure baseline rotation rate using the Sagnac effect, and are potentially very sensitive. These are described in more detail elsewhere (references), but impose some constraints on the configuration – they do not work for systems arrayed in a planar configuration perpendicular to the target direction, for example.

The analysis above has implicitly assumed that the beam shear is zero; small drifts in the beam shear will lead to errors in delay and delay rate estimation. Equations (3) and (4) are specific to the geometry shown in Fig. 3, but can be adapted in a straightforward way to different geometries. Indeed, the analysis above also applies to structurally connected interferometers.

7. FUTURE MISSIONS

Mission	Goal	Wavelength	Baselines	Apertures	Angular resolution	Observation mode (see Table 1)
StarLight	Technology precursor for TPF	Visible 0.6 – 1.0 μm	30 – 125 m	2 x 12 cm	1 mas	Visibility amplitude
Terrestrial Planet Finder	Detect earth-like planets around nearby stars + astrophysics	Mid-IR 7 – 20 μm	25 – 1000 m	4 x 3.5 m	2 mas	Nulling & Imaging
SMART 2 & 3	Technology precursor for DARWIN & LISA	N/A	N/A	N/A	N/A	Metrology only?
DARWIN	Detect earth-like planets around nearby stars + astrophysics	Mid-IR 7 – 20 μm	25 – 1000 m	6 x 1.5 m	2 mas	Nulling, Imaging
SPECS	Submillimeter Probe of the Evolution of Cosmic Structure	Submm – Far IR 40 - 500 μm	< 1 km	3 x 3 m	50 mas	Imaging
Stellar Imager	Image surface activity on nearby stars	UV	<500 m	10-30 x 1 m	~100 μas	Imaging
MAXIM	Micro-Arcsecond Xray Imaging Mission	X-Ray	100 m	33 x ?	0.3 μas	Imaging
MAXIM Pathfinder	Precursor for MAXIM	X-Ray	1.4 m	100 cm^2	100 μas	Imaging
Life Finder	Search for spectral signatures of life on other planets	Visible / infrared	100 m	4 x 25 m	~ 20 mas	Nulling
Planet Imager	25 x 25 pixels across Earth-like planet	Visible / infrared	400 km	25 x 40 m	~ 1 μas	Nulling

Table 3: Summary of goals and key parameters for selection of future formation flying interferometer missions. Numbers are approximate only.

Much of the recent work on formation flying interferometry has been driven by NASA's Terrestrial Planet Finder and ESA's DARWIN mission. The primary goal for each is to directly detect Earth-like planets around nearby stars. The longer baselines (>200 m) are motivated by the higher resolution needs of imaging other interesting astrophysical objects. Formation-flyers offer adjustable baseline lengths to tune the response to the planetary system under study, and longer baselines than fixed structures capable of observing more distant systems. Other non-formation-flying architectures are under consideration for TPF; a structurally connected interferometer operating in the mid-IR, and a coronagraph operating at visible wavelengths. There are technology precursors associated with both TPF and DARWIN. NASA's StarLight mission is intended to demonstrate formation flying and optical interferometry, using two spacecraft (references). The flight development activities of StarLight were terminated in March 2002, late in the project Mission and System Definition Phase. Since then, the StarLight project has been merged with the TPF Project and will continue to develop ground technologies for formation-flying interferometry. ESA's SMART-2 and SMART-3 serve a similar purpose, but the detailed implementation remains to be defined.

The SPECS mission operates at submillimeter and far-IR wavelengths. Current plans use a system of tethers to help maintain the formation with baselines out to 1 km. The collectors are large flats, which deflect the beams to a central combining hub. Another innovation is the use of imaging Fourier Transform Spectroscopy; the inputs from the collectors are combined in the pupil plane and imaged over a number of pixels in the focal plane to obtain a wide field of view. The relative delay of the beams is then adjusted to measure the fringe visibility in each pixel as a function of delay, which can be inverted to give the spectrum.

The Stellar Imager mission requires long baselines at UV wavelengths to resolve sunspots and surface activity on other stars. Designs using both pupil-plane combination (aka Michelson) with a small number of collectors, and image-plane combination (aka Fizeau) with a large number of detectors have been considered. High resolution imaging drives the need for a formation flying interferometer.

MAXIM, and its precursor MAXIM Pathfinder are ambitious X-Ray interferometer missions, where the ultimate goal is to image black-hole event horizons with sub-microarcsecond resolution. Since the wavelength is extremely short (~1 nm), the baseline lengths required are relatively modest. The grazing incidence optics required for operation at X-Ray wavelengths demand that the combiner spacecraft is located at a great distance (500 km) behind the collectors, and station-keeping requirements are extremely tight. The currently proposed Pathfinder mission houses a ring of collectors within a single spacecraft, which redirect the light to a combiner spacecraft at a distance of 500 km.

Life Finder and Planet Imager build on the technologies of previous missions to realize the long-term goals of searching for extra-terrerstrial life by characterizing potentially habitable planets both spectrally (Life Finder) and spatially (Planet Imager). Formation flying interferometry is currently seen as the only feasible approach to meeting the demands of sensitivity and angular resolution needed to rise to these challenges.

This research was carried out at the Jet Propulsion Laboratory, California Institute of Technology, under a contract with the National Aeronautics and Space Administration. Reference herein to any specific commercial product, process, or service by trade name, trademark, manufacturer, or otherwise, does not constitute or imply its endorsement by the United States Government or the Jet Propulsion Laboratory, California Institute of Technology.

REFERENCES

Gary StarLight paper
Riley StarLight paper
KOG reference (old SPIE?)
Gyro paper, this conference
TPF book
http://sci.esa.int/home/darwin/index.cfm

http://space.gsfc.nasa.gov/astro/specs/
http://hires.gsfc.nasa.gov/~si/
http://maxim.gsfc.nasa.gov/docs/vision.html
http://maxim.gsfc.nasa.gov/docs/pathfinder/pathfinder.html